

**Ni-Ce-OMS-2 material: preparation and preliminary catalytic-study
on removing ethanol in the gas phase**

Gia-Han Nguyen^{1,2}, Quoc-Long Dang-Hung^{1,2}, Trong-Phu Tran^{1,2}, Dung V. Nguyen^{1,2},
Long Q. Nguyen^{1,2} and Tuyet-Mai Tran-Thuy^{1,2*}

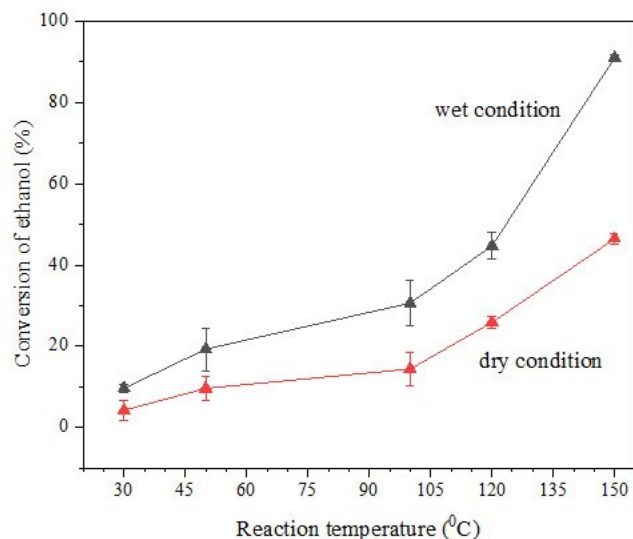
¹ Faculty of Chemical Engineering, Ho Chi Minh City University of Technology
(HCMUT), 268 Ly Thuong Kiet Street, District 10, Ho Chi Minh City, Viet Nam

² Vietnam National University Ho Chi Minh City, Linh Trung Ward, Thu Duc City, Ho
Chi Minh City, Viet Nam

*Corresponding author: Tuyet-Mai Tran-Thuy

E-mail: tuyetmai@hcmut.edu.vn

GRAPHICAL ABSTRACT



ABSTRACT

Cryptomelane type manganese oxide K-OMS-2 and Ni-Ce-OMS-2 co-doping materials were synthesized by one-step preparation with refluxing system. The crystalline structure, and morphology were characterized by X-ray diffraction analysis and SEM images. Ni (II) and Ce (III) were incorporated into cryptomelane, substituted for Mn (III) and Mn (IV) resulting an increase of Mn-average-oxidation-state from 3.6 to 3.8 for un-doped and co-doped samples, respectively. With different amount of precursor-cerium concentration, NiCe1.0 improved the ethanol conversion by a factor of 8 compared to unmodified K-OMS-2. Additionally, NiCe1.0 showed a significant increase of ethanol conversion with reaction temperature. Over above 90% of ethanol was total oxidized at 150 °C suggesting a potential Ni-Ce-OMS-2 catalyst for removing volatile organic compounds at low temperature.

Keywords: Ni-Ce-OMS-2; Ni-Ce-cryptomelane; removing ethanol vapor; manganese AOS; deep oxidation of ethanol

1. Introduction

The rapid growth of human population, urbanization and industrialization have greatly contributed to the volatile organic compounds (VOCs) emission threatening our living-environment [Kamal *et al.*, 2016]. VOCs are classified as indoor air pollutants causing many detrimental effects on both the environment and human health [Kamal *et al.*, 2016 and Møhlhave *et al.*, 1991]. CO was concerned as indoor air pollutant which is deadly poisonous when inhaled in large amount [Zhou *et al.*, 2014]. Formaldehyde can cause illness, soreness of the eyes, nose and throat, even at low levels or short periods [Robert *et al.*, 2021]. Long-term exposure to toluene has been reported to suffer from neurological disorders [Kyzas *et al.*, 2022]. Ethanol, which is one of the most common VOCs, is widely presented in industrial and consumer products such as dyes, inks, polishes, biofuels, cosmetics, perfumes, etc [Li *et al.*, 2020]. Moreover, due to Covid-19 pandemic, the use of alcohol-based hand rubs or ethanol 70% for sterilization significantly surges in homes, medical centers and hospitals. Exposing to high level of ethanol vapor for long period time causes headache, irritation of mucous membrane, lack of concentration and drowsiness [Hautemanière *et al.*, 2013 and Criddle *et al.*, 2019]. At present, various technologies of VOCs treatment have been applied, namely adsorption, thermal oxidation and catalytic oxidation [Zhu *et al.*, 2020, He *et al.*, 2019 and Khan *et al.*, 2000]. Among them, the most feasible and energy-saving approach to remove VOCs under mild operating conditions is

oxidation catalysis. Nowadays, metal oxide-based catalyst is being used thanks to its cost-effectiveness, less toxicity, also having good thermal stability and high surface area. And manganese oxide-based catalysts are known as low-cost materials exhibiting high activity of VOCs total oxidation [He *et al.*, 2019, Khan *et al.*, 2000, Luo *et al.*, 2000 and Dinh *et al.*, 2021].

Manganese oxides, an octahedral molecular sieve (OMS), have been much attracted as a promising catalyst due to their acceptable cost, high catalytic performance compared to noble metal ones [Suib *et al.*, 2008 and Gandhe *et al.*, 2007]. This material has manganese oxides framework with structural unit of MnO_6 octahedra connecting by sharing vertices and edges, creating a tunnel structure. The OMS materials are varied through the arrangement of MnO_6 octahedra units that define the tunnel structure with dimensions ranging from $(2.3 \times 2.3) \text{ \AA}$ to $(4.6 \times 11.5) \text{ \AA}$ [Sabaté *et al.*, 2021]. Manganese oxide octahedral molecular sieve cryptomelane (K-OMS-2) is an one-dimensional manganese oxide, formed a 2×2 tunnel structure having dimensions of 4.6 \AA with K^+ ions inside for a charge balance system [Yin *et al.*, 1994].

The modification of cryptomelane by doping foreign metal cations could tune the physicochemical properties assigned to creation of more surface defects and oxygen vacancies [18]. Different cations such as Cr^{3+} , Ce^{3+} , Co^{2+} , Ni^{2+} and Ag^+ have been substituted successfully into the OMS-2 structure for a promotion of catalytic performance [Tran *et al.*, 2012, Tran-Thuy *et al.*, 2021, Huang *et al.*, 2020 and Sun *et al.*, 2014]. However, studies on modification of the cryptomelane surface with two dopants (co-

doping cryptomelane) are still little concerns. In this work, nickel and cerium will be co-doped into cryptomelane structure via one-step preparation and the oxidation catalysis in removal of ethanol vapor will be investigated.

2. Materials and methods

2.1. Preparation of K-OMS-2 and Ni-Ce-OMS-2 materials

All chemicals were purchased from Shanghai Zhanyun Chemical Co., Ltd and Duc Giang Detergent-Chemical JSC, Vietnam without further purification. A solution of Mn^{2+} , Ni^{2+} and Ce^{3+} cations was mixed with potassium permanganate at room temperature, at $\text{pH} < 2$. Typically, 1.0 M of Ni^{2+} cation in the reactant mixture and 1.4 of the molar ratio of Mn^{2+} and Mn^{7+} were prepared before that. Amount of Ce^{3+} cations in the precursor mixture was adjusted with 1.0 and 1.5 M; correspondingly to NiCe1.0 and NiCe1.5 for the received-final products. The mixture was further refluxed in a one-step at 100 °C for 24 hours. After that, the brown slurry was washed many times with distilled water, filtered and dried overnight at 120 °C. For a comparison, an un-doped cryptomelane (K-OMS-2, K0) was prepared following the protocol reported in our previous work [Tran-Thuy *et al.*, 2021].

2.2 Material characterization analysis

The materials' characteristics were analyzed using XRD, SEM, AOS, and ICP-MS methods. X-ray diffraction analysis was carried out on a Bruker D8 Advance diffractometer using $\text{Cu-K}\alpha$ radiation. Morphologies were analyzed by using a Hitachi-S4800 FE-SEM for scanning electron microscopy. The chemical composition was determined by the

inductively coupled-plasma mass spectrometry (ICP-MS, Optima™ 8000 ICP-OES). The manganese average oxidation state (Mn-AOS) was determined by titration method [Tran-Thuy *et al.*, 2021].

2.3 Catalytic performance testing

The catalytic testing in ethanol total oxidation was conducted under atmospheric pressure in a glass fix-bed reactor, which was placed in an electric furnace connected to a reaction temperature controller. Typically, 0.05g of catalyst and 0.05g of SiO₂ quartz were mixed and loaded in the reactor.

Ethanol vapor was carried by adding an inert nitrogen gas into an impinger containing absolute ethanol kept at 0 °C. The ethanol vapor flow was mixed with a pure O₂ flow and another N₂ one passing through a water tank maintained at 30 °C to simulate an airflow with flowrate of 50 mL/min and relative humidity (RH) of 20%. The feeding flow was introduced in the reactor and the reaction temperature was controlled in the range of 30-150 °C by a water bath. Ethanol vapor removal efficiency (H_{Eth}%) was calculated as the following equation:

$$H_{Eth}\% = \frac{[EtOH]_{in} - [EtOH]_{out}}{[EtOH]_{in}} \times 100\% \quad (1)$$

Wherein, [EtOH]_{in} and [EtOH]_{out} are representative for the concentration of ethanol in the inlet and outlet gas stream of the reactor.

3. Results and Discussion

3.1. Characterizations of catalysts

The elemental compositions of synthesized materials from ICP-MS analysis are displayed in Table 1. The K, Mn, Ni and Ce elements were all presented in the Ni-Ce-OMS-2 samples. When the cerium precursor concentration rose from 0.1 to 0.15M, the manganese content in NiCe1.0 and NiCe1.5 decreased from 49.8 to 44.9 wt.%. The manganese percentage of these samples were noticeable dropped when compared with ~59 wt.% of manganese for un-doped cryptomelane K0 sample. The dopants Ni and Ce greatly reduced the amount of potassium ion presenting in the tunnels of OMS-2 structure since the molar ratio of potassium over manganese elements dropped from 0.86/8 (K0 sample) to 0.40/8 (NiCe1.5 sample). Consistently, molar ratio of cerium and manganese increased from 0.43/8 to 0.71/8 for NiCe1.0 and NiCe1.5, respectively. The amount of nickel dopant was recorded at constant value as 0.02/8 of the molar ratio of nickel over manganese, regarding to the same nickel precursor concentration in preparation of co-doping samples.

Figure. 1 shows that K0, NiCe1.0, NiCe1.5 samples have all the signature diffraction patterns at 2θ of 12.6° , 17.9° , 28.7° , 37.5° , 41.9° , 49.9° and 60.1° ; representing the cryptomelane structure (JCPDS 29-1020). Nickel and cerium dopants created some interferences in the diffractogram picture resulting broader and shorter peaks over NiCe1.0, NiCe1.5 samples in comparison to the un-doped one. This indicates the cerium loading affects the cryptomelane crystal of synthesized materials.

Table 1. ICP – MS results and Mn-AOS of synthesized materials

Sample	ICP analysis		Mn-AOS	Ref.
	Mn [wt%]	Molar ratio $n_K/n_{Mn}/n_{Ce}/n_{Ni}$		
K0	59.59	0.86/8/ - / -	3.60	[14]
NiCe1.0	49.80	0.65/8/0.43/0.02	3.83	This work
NiCe1.5	44.88	0.40/8/0.71/0.02	3.84	This work

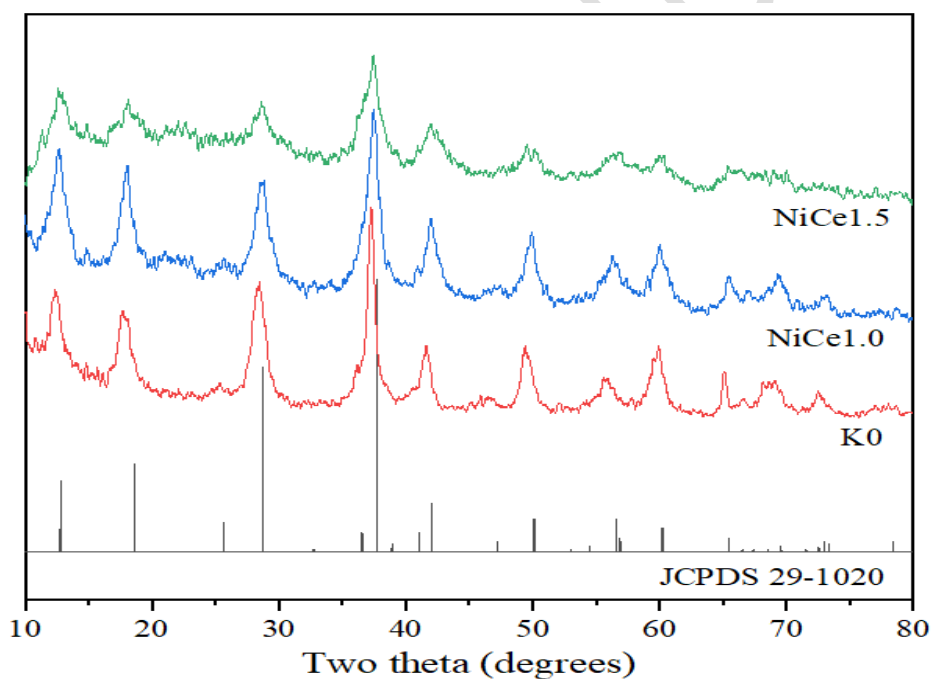


Figure 1. XRD patterns of OMS-2 materials

The Mn-AOS (as shown in Table 1) of NiCe1.0 and NiCe1.5 samples increased to around 3.8 comparing to 3.6 of the un-doped K0 sample possibly performing a partial replacement of Ni^{2+} and Ce^{3+} for lower oxidation state of manganese sites. This consisted with increase

of chromium loading resulting an incline of Mn-AOS over Cr-doped cryptomelane. This also figured out that chromium dopant took part in weakening the Mn-O bonds leading a positive effect on enhancement of formaldehyde-total oxidation [Tran-Thuy *et al.*, 2021].

SEM images for Ni-Ce-OMS-2 materials are shown in Figure. 2 and Figure. 3, respectively. K-OMS-2 prepared by reflux method have nanorod-like morphology [Wang *et al.*, 2009] which are agglomerated as clusters in the presence of nickel and cerium for preparation of cryptomelane. These clusters distribute randomly, not in any certain order, creating numerous voids in Ni-Ce-OMS-2 samples. The surface morphology of OMS-2 materials remains unchanged nanorod-like over NiCe1.0 sample ($n_{\text{Ce}}/n_{\text{Mn}} = 0.41/8$) having diameter at 20 ± 5 nm agglomerating into many clusters with the average size at 436 ± 19 nm (Figure 4a and Figure 4b) [Wang *et al.*, 2009 and Dong *et al.*, 2021]. When increasing the percentage of cerium loading in NiCe1.5 sample ($n_{\text{Ce}}/n_{\text{Mn}} = 0.71/8$), the clusters are clearly observed with various sizes, ranging from 200 nm to 2000 nm with the average diameter at 550 ± 58 nm (Figure 4c) and the nanorod-like shape disappears due to a slight aggregation (Figure. 3).

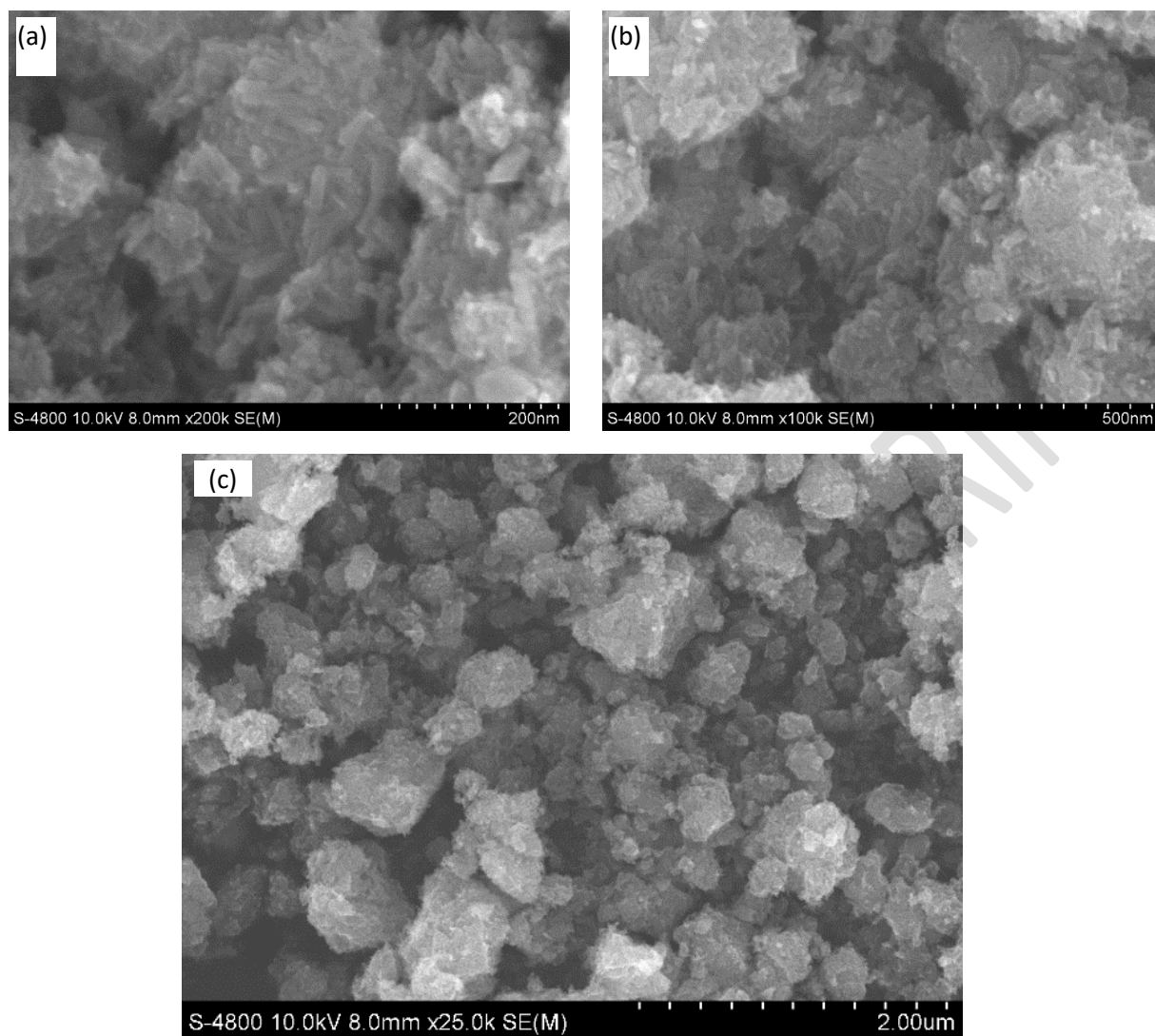


Figure 2. SEM images of NiCe1.0 samples at (a) 200 nm, (b) 500 nm and (c) 2 μ m of scales

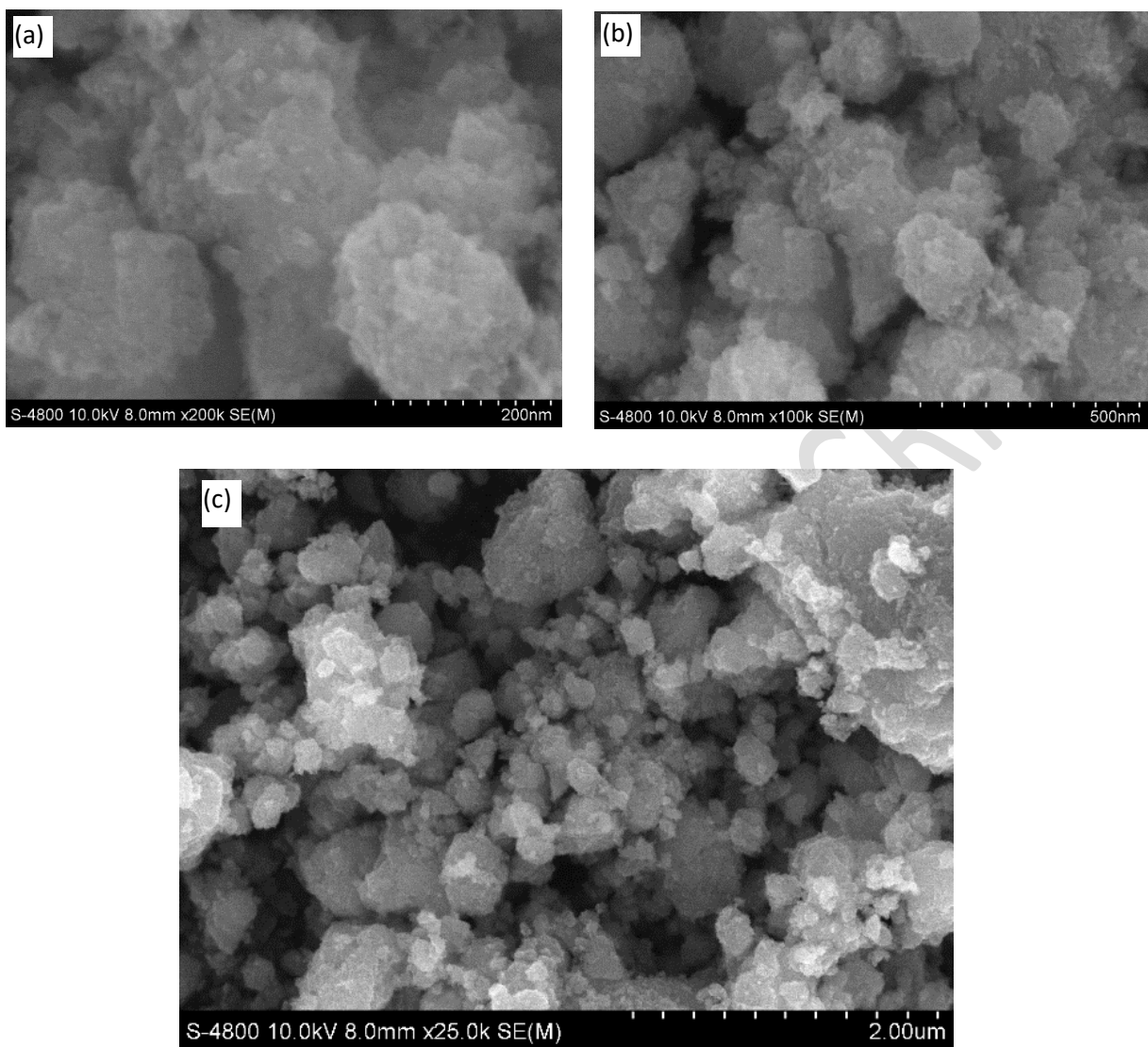


Figure 3. SEM images of NiCe_{1.5} samples at (a) 200 nm, (b) 500 nm and (c) 2 μm of scales

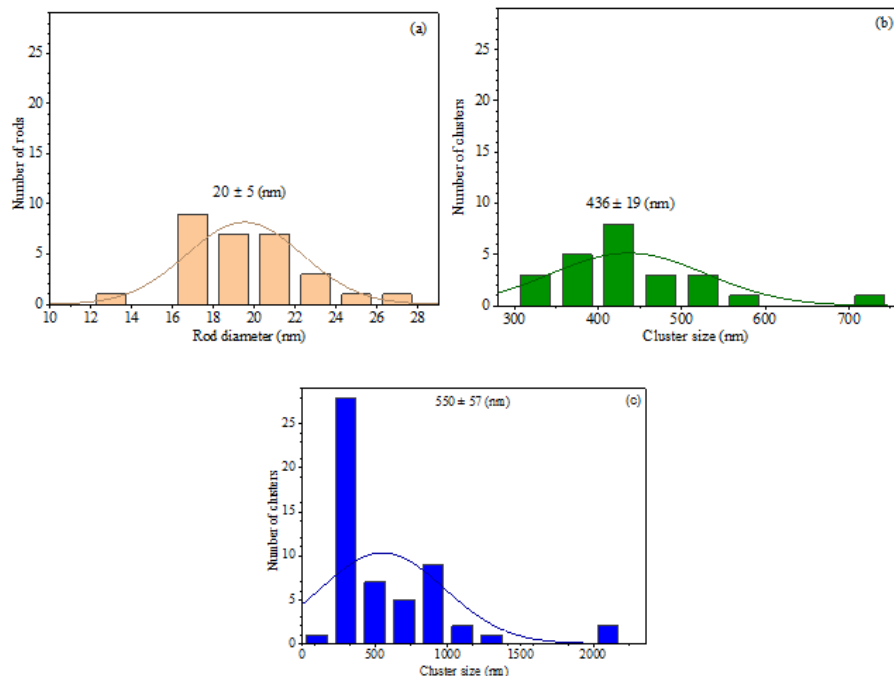


Figure 4. Size distributions of (a) nanorods, (b) clusters from NiCe1.0 material and (c) that of clusters from NiCe1.5 sample

3.2. Removal of ethanol vapor by K-OMS-2 and modified cryptomelane catalysts

A skimming investigation of ethanol oxidation shows that K0 and NiCe1.5 materials had no efficiency in oxidizing ethanol vapor as less than 3.0% of removed ethanol during reaction at 30 °C. However, the NiCe1.0 presents a remarkable performance in removing ethanol vapor at 30 °C of reaction temperature, which is $9.6 \pm 1.0 \%$. This indicates the worth effect of Ni and Ce co-dopant in the cryptomelane structure and a certain amount of the dopants dominates the catalytic activity. Figure. 5 presents the incline of NiCe1.0-catalytic performance versus the reaction temperature. $19 \pm 5.2 \%$ of ethanol vapor removal efficiency ($H_{\text{Eth}}\%$) is recorded at 50 °C and the $H_{\text{Eth}}\%$ gets $44.6 \pm 3.3 \%$ at 120 °C of the

reaction temperature. The notable increase in $H_{\text{Eth}}\%$ to $91 \pm 0.8 \%$ could be observed at 150 °C of the reaction temperature revealing a possible NiCe1.0 catalyst in ethanol deep-oxidation at low temperature. It was reported that less than 25% of ethanol was total converted on Mn-Cu oxide catalysts [Morales et al., 2006] and only ~5% of ethanol was total oxidized over manganese oxide catalyst [Bastos et al., 2009] at 150 °C of oxidation temperature. This evidences a comparable NiCe1.0 material for efficient removal of VOCs, in general and in particular of ethanol vapor at low temperature.

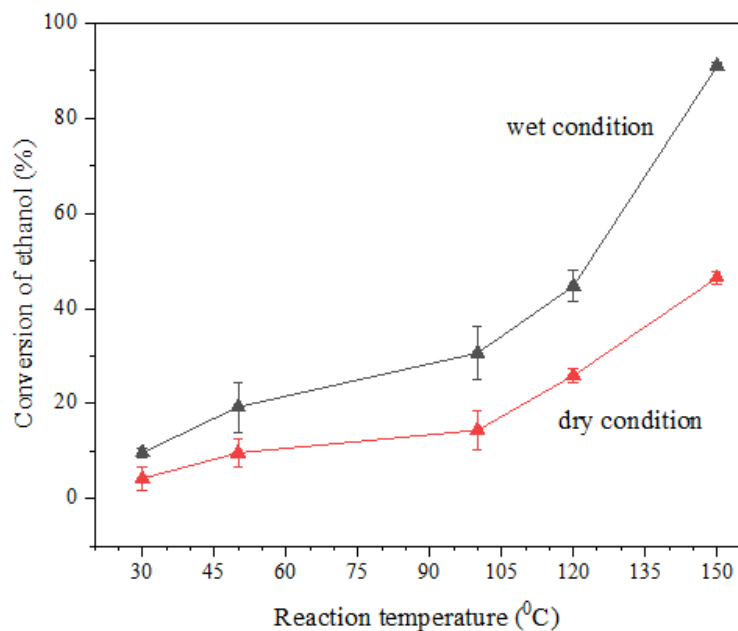


Figure 5. Ethanol conversion on NiCe1.0 catalyst at different reaction temperature

4. Conclusions

The co-doped Ni-Ce-OMS-2 materials are synthesized via one-step method in the assistance of reflux system. SEM images show the aggregation of cryptomelane nanorod-like morphology after loading Ni and Ce dopants to the K-OMS-2 structure. The dopants

also give rise to AOS of manganese from 3.60 to around 3.80, showing that Ni and Ce dopants partly take over the positions of manganese with lower oxidation state in the OMS-2 framework. The ethanol vapor conversion over NiCe1.0 is enhanced compared to the undoped K-OMS-2. At 150 °C of the reaction temperature, the co-doped catalyst effectively removes over 90% ethanol in the feeding stream.

Acknowledgment

This research is funded by Vietnam National University HoChiMinh City (VNU-HCM) under grant number: B2023-20-21. We acknowledge the support of time and facilities from Ho Chi Minh City University of Technology.

References

- Bastos S.S.T., Órfão J.J.M., Freitas M.M.A., Pereira M.F.R., Figueiredo J.L. (2009), Manganese oxide catalysts synthesized by exotemplating for the total oxidation of ethanol, *Applied Catalysis B: Environmental*, **93(1–2)**, 30–37. DOI: 10.1016/J.APCATB.2009.09.009.
- Criddle W.J., Koziel J., Van-Leeuwen H., Jenks W. (2019), Ethanol, *Encyclopedia of Analytical Science (Third Edition)*, **3**, 39–46. DOI: 10.1016/B978-0-12-409547-2.14560-3.
- Dinh M.T.N., Nguyen C.C., Phan M.D., Duong M.K., Nguyen P.H.D., Lancelot C., Nguyen D.L. (2021), Novel cryptomelane nanosheets for the superior catalytic

combustion of oxygenated volatile organic compounds, *Journal of Hazardous Materials*, **417**, 126111. DOI: 10.1016/J.JHAZMAT.2021.126111.

Dong N., Chen M., Ye Q., Zhang D., Dai H. (2021), Catalytic Elimination of Carbon Monoxide, Ethyl Acetate, and Toluene over the Ni/OMS-2 Catalysts, *Catalysts*, **11(5)**, 581. DOI: 10.3390/catal11050581.

Gandhe A.R., Rebello J.S., Figueiredo J.L., Fernandes J.B. (2007), Manganese oxide OMS-2 as an effective catalyst for total oxidation of ethyl acetate, *Applied Catalysis B: Environmental*, **72(1–2)**, 129–135. DOI: 10.1016/J.APCATB.2006.10.017.

Hautemanière A., Cunat L., Ahmed-Lecheheb D., Hajjard F., Gerardin F., Morele Y., Hartemann P. (2013), Assessment of exposure to ethanol vapors released during use of Alcohol-Based Hand Rubs by healthcare workers, *Journal of Infection and Public Health*, **6(1)**, 16–26. DOI: 10.1016/J.JIPH.2012.09.015.

He C., Cheng J., Zhang X., Douthwaite M., Pattison S., Hao, Z. (2019), Recent Advances in the Catalytic Oxidation of Volatile Organic Compounds: A Review Based on Pollutant Sorts and Sources, *Chemical Reviews*, **119**, 4471–4568. DOI: 10.1021/acs.chemrev.8b00408.

Huang Y., Yan J., Zhang, N., Zheng K., Hu Y., Liu X., Meng X. (2020), The Effect of Metal Ions as Dopants on OMS-2 in the Catalytic Degradation, *Catalysis Letters*, **150(7)**, 2021–2026. DOI: 10.1007/s10562-020-03123-0.

Kamal M.S., Razzak S.A., Hossain M.M. (2016), Catalytic oxidation of volatile organic compounds (VOCs) – A review, *Atmospheric Environment*, **140**, 117–134. DOI: 10.1016/J.ATMOSENV.2016.05.031.

Khan F.I., Ghoshal, A.K. (2000), Removal of Volatile Organic Compounds from polluted air, *Journal of Loss Prevention in the Process Industries*, **13(6)**, 527–545. DOI: 10.1016/S0950-4230(00)00007-3.

Kyzas G.Z., McKay G., Al-Musawi T.J., Salehi S., Balarak D. (2022), Removal of Benzene and Toluene from Synthetic Wastewater by Adsorption onto Magnetic Zeolitic Imidazole Framework Nanocomposites, *Nanomaterials*, **12(17)**, 3049. DOI: 10.3390/nano12173049.

Li Y., Cao D., Jia F.A., Chang F., LV R., Dai J. K. (2020), Preparation of natural pyrethrum-poly(lactic acid) microspheres with different particle sizes and surface morphology, *Materials Letters*, **264**, 127345. DOI: 10.1016/J.MATLET.2020.127345.

Luo J., Zhang Q., Huang A., Suib S.L. (2000), Total oxidation of volatile organic compounds with hydrophobic cryptomelane-type octahedral molecular sieves, *Microporous and Mesoporous Materials*, **35–36**, 209–217. DOI: 10.1016/S1387-1811(99)00221-8.

Mølhav L. (1991), Volatile Organic Compounds, Indoor Air Quality and Health, *Indoor Air*, **1(4)**, 357–376. DOI: <https://doi.org/10.1111/j.1600-0668.1991.00001.x>.

- Morales M.R., Barbero B.P., Cadús L.E. (2006), Total oxidation of ethanol and propane over Mn-Cu mixed oxide catalysts, *Applied Catalysis B: Environmental*, **67(3–4)**, 229–236. DOI: 10.1016/J.APCATB.2006.05.006.
- Robert B., Nallathambi G. (2021), Indoor formaldehyde removal by catalytic oxidation, adsorption and nanofibrous membranes: a review, *Environmental Chemistry Letters*, **19**, 2551–2579. DOI: 10.1007/s10311-020-01168-6.
- Sabaté F., Sabater M.J. (2021), Recent Manganese Oxide Octahedral Molecular Sieves (OMS–2) with Isomorphically Substituted Cationic Dopants and Their Catalytic Applications, *Catalysts*, **11(10)**, 1147. DOI: 10.3390/catal11101147.
- Suib S.L. (2008), Porous Manganese Oxide Octahedral Molecular Sieves and Octahedral Layered Materials, *Accounts of Chemical Research*, **41(4)**, 479–487. DOI: 10.1021/ar7001667.
- Sun H., Qiu G., Wang Y., Feng X., Yin H., Liu, F. (2014), Effects of Co and Ni co-doping on the physicochemical properties of cryptomelane and its enhanced performance on photocatalytic degradation of phenol, *Materials Chemistry and Physics*, **148(3)**, 783–789. DOI: 10.1016/J.MATCHEMPHYS.2014.08.049.
- Tran T.-P., Ta-Thi X.-P., Nguyen K.-C., Tran D.-N., Nguyen-Phan T.-D., Pham K.-N., Nguyen G.-H., Tran-Thuy T.-M. (2021), Enhanced formaldehyde-removal over modified cryptomelane catalysts, *IOP Conference Series: Earth and Environmental Science*, **947(1)**, 012024. DOI: 10.1088/1755-1315/947/1/012024.

Tran-Thuy T.M., Le T.P., Tran, T.P., Lam H.H., Nguyen L.Q., Nguyen D. V., Dang-Bao T. (2021), Chromium-doped cryptomelane: Mn-O debilitation and reactive enhancement in formaldehyde abatement, *Materials Letters*, **305**, 130777. DOI: 10.1016/J.MATLET.2021.130777.

Wang R., Li J. (2009), OMS-2 Catalysts for Formaldehyde Oxidation: Effects of Ce and Pt on Structure and Performance of the Catalysts, *Catalysis Letters*, **131(3)**, 500–505. DOI: 10.1007/s10562-009-9939-5.

Yin Y.-G., Xu W.-Q., DeGuzman R., Suib S.L., O'Young C.L. (1994), Studies of Stability and Reactivity of Synthetic Cryptomelane-like Manganese Oxide Octahedral Molecular Sieves, *Inorganic Chemistry*, **33(19)**, 4384–4389. DOI: 10.1021/ic00097a029.

Zhou Y., Wang Z., Liu C.-J. (2014), Perspective on CO oxidation over Pd-based catalysts, *Catalysis Science & Technology*, **5**, 69–81. DOI: 10.1039/C4CY00983E.

Zhu L., Shen D., Luo K.H. (2020), A critical review on VOCs adsorption by different porous materials: Species, mechanisms and modification methods, *Journal of Hazardous Materials*, **389**, 122102. DOI: 10.1016/J.JHAZMAT.2020.122102.